

SARNet: A SPIKE-AWARE CONSECUTIVE VALIDATION FRAMEWORK FOR ACCURATE REMAINING USEFUL LIFE PREDICTION

Junhao Fan^{1†}, Wenrui Liang^{2†}, Wei-Qiang Zhang^{2*}

¹Georgetown University, Washington, DC, USA

²Department of Electronic Engineering, Tsinghua University, Beijing, China

jf1687@georgetown.edu, wqzhang@tsinghua.edu.cn

ABSTRACT

Accurate prediction of remaining useful life (RUL) is essential to enhance system reliability and reduce maintenance risk. Yet many strong contemporary models are fragile around fault onset and opaque to engineers: short, high-energy spikes are smoothed away or misread, fixed thresholds blunt sensitivity, and physics-based explanations are scarce. To remedy this, we introduce **SARNet** (Spike-Aware Consecutive Validation Framework), which builds on a Modern Temporal Convolutional Network (ModernTCN) and adds spike-aware detection to provide physics-informed interpretability. ModernTCN forecasts degradation-sensitive indicators; an adaptive consecutive threshold validates true spikes while suppressing noise. Failure-prone segments then receive targeted feature engineering (spectral slopes, statistical derivatives, energy ratios), and the final RUL is produced by a stacked RF-LGBM regressor. Across benchmark-ported datasets under an event-triggered protocol, SARNet consistently lowers error compared to recent baselines (RMSE 0.0365, MAE 0.0204) while remaining lightweight, robust, and easy to deploy.

Index Terms— Remaining useful life (RUL), predictive maintenance, modern temporal convolutional networks (MTCN), spike-aware onset detection

1. INTRODUCTION

Remaining useful life (RUL) prediction is central to predictive maintenance, especially for bearings whose degradation can accelerate after onset. [1–3] Classical statistical thresholds rarely cope with the non-linear, condition-dependent dynamics seen in practice [4–6].

Recent research spans both event detection and deep sequence modeling. Chen and Tian [7] use a prototypical network to detect critical points (sudden degradation) and then switch to RUL prediction, updating the reference state over time. Yao et al. [8] build Patch ModernTCN-Mixer, a dual-task network that couples first prediction time (FPT) detection with RUL using a dynamic semi-soft threshold and GradNorm. Other pipelines pair signal denoising and hand-crafted health indices with recurrent predictors. For example, Zou et al. [9] denoise with DWT, rank the candidate features, compress them with KPCA, and then feed the resulting embeddings to an attention-DBiLSTM, achieving strong cross-dataset robustness. Convolutional approaches further improve accuracy [10–12]. A TCN with causal dilations plus multi-head self-attention reweights

the global context for rolling-bearing RUL [13, 14]; end-to-end multi-channel CNNs, optionally followed by attention LSTM, deliver strong MAE/RMSE from raw signals [15].

However, three practical gaps persist. First, fixed spike rules (e.g., $x+3\sigma$) are noise-sensitive and often trigger prematurely [16]. Second, even strong deep features usually require calibration to yield stable post-onset RUL when degradation evidence is sparse [17]. Third, results on bearing life prediction should have the opportunity to be applied in real-life conditions. However, although most deep learning models and other models have accurate prediction results, they lack model interpretability and are difficult to deploy in real life. [18–20]

SARNet addresses both issues with an event-triggered, two-stage design. A Modern Pure Convolution Structure for General Time Series (MTCN) [21] first forecasts a degradation-sensitive indicator; an *adaptive consecutive-spike* rule then confirms sustained onset before prognosis. Unlike prior first-prediction time (FPT) detectors by Yao et al., our rule demands d_{\min} consecutive exceedances and *falls back* to full-sequence prediction when spike evidence is weak, reducing false alarms without sacrificing coverage. For the post-onset segment, we replace a single heavy predictor with a lightweight, interpretable RF-LGBM ensemble head, providing calibrated estimates and feature attributions. By separating forecasting, onset validation, and calibrated regression, we concentrate learning where it matters most, reduce sensitivity to noise, and keep the whole pipeline interpretable.

Contributions are listed below:

- **Event-triggered formulation.** Rather than one-shot RUL regression, ModernTCN forecasts a degradation indicator $\hat{z}_{t+h} = f_{\theta}(x_{t-L+1:t})$. A spike-aware detector declares onset only if

$$T_t = \bigwedge_{i=0}^{K-1} (\hat{z}_{t-i} > \tau_t), \quad \tau_t = \mu_t + k_{\sigma} \sigma_t,$$

with a small hysteresis to avoid chattering. This *consecutive*, *adaptive* rule encodes impact-induced transients observed in vibration signals, tying triggers to fault physics and making the subsequent RUL estimation interpretable and robust across conditions.

- **Robust onset validation.** An adaptive consecutive-spike rule with a simple fallback (when evidence is weak) confirms onset, making the trigger far less noisy than fixed $x + 3\sigma$ thresholds.

† Equal contribution. *Corresponding author.

This work was supported by the National Natural Science Foundation of China under Grant No. 62276153.

- **Calibrated and interpretable prognosis.** After onset is validated, a lightweight, interpretable RF-LGBM head delivers calibrated post-onset RUL with clear importance of characteristics, facilitating real engineering use.

2. METHODOLOGY

This study proposes the SARNet to predict the remaining useful life (RUL). The framework integrates a Modern Temporal Convolutional Network (ModernTCN), an adaptive spike detection mechanism, and ensemble regression models. Figure 1 provides an overview of the pipeline.

The raw sensor signals are denoted as $x_t \in \mathbb{R}$, where t indexes discrete time steps with a sampling interval of $\Delta t = 60$ seconds.

To identify the most degradation-sensitive feature, we computed the absolute Spearman correlation between each engineered feature and the ground-truth RUL under all operating conditions. As shown in Table 1, `FFT_bin_2_H`, which is denoted as the value extracted from the second frequency bin of the magnitude of FFT of the horizontal signal, achieved the highest absolute correlation, making it the main indicator used for subsequent modeling.

Feature Name	Absolute Spearman Correlation
<code>FFT_bin_2_H</code>	0.535
<code>Skewness_H</code>	0.302
<code>FFT_bin_5_H</code>	0.301
<code>BandPower_Mid_V</code>	0.272
<code>Kurtosis_V</code>	0.242
<code>BandPower_Mid_H</code>	0.203
<code>RMS_V</code>	0.202
<code>Kurtosis_H</code>	0.182
<code>FFT_bin_4_V</code>	0.179
<code>CrestFactor_H</code>	0.168

Table 1: Top 10 sensor features ranked by absolute Spearman correlation with RUL.

In this research, each feature is normalized using min-max scaling:

$$x_t^{\text{norm}} = \frac{x_t - \min(x)}{\max(x) - \min(x)}, \quad (1)$$

where $\min(x)$ and $\max(x)$ are calculated in the training set to avoid data leakage. The data set is then divided into training and testing partitions, ensuring that there is no temporal overlap between them.

2.1. Adaptive Consecutive Spike Detection

Accurate detection of degradation onset is critical for reliable RUL prediction, particularly under varying operating conditions where transient noise may cause false alarms. Conventional thresholding methods, such as the fixed $x + 3\sigma$ rule [22], treat any single exceedance as an anomaly, making them highly sensitive to random fluctuations.

Our new model, SARNet, overcomes this limitation and provides mechanism-level interpretability consistent with engineering and physical principles.

2.1.1. Adaptive Thresholding

Given a predicted degradation-sensitive feature sequence $\{\hat{y}_t\}_{t=1}^T$, the adaptive threshold θ is defined as:

$$\theta = \mu_{\text{ref}} + k\sigma_{\text{ref}}, \quad k = 2 \quad (2)$$

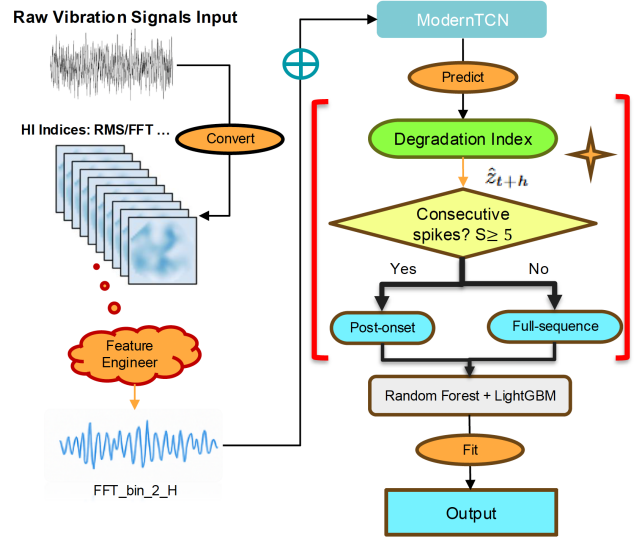


Fig. 1: The SARNet Framework

where μ_{ref} and σ_{ref} are the mean and standard deviation computed from a reference (healthy) operating window, and k is a sensitivity coefficient. Compared to the traditional $k = 3$ setting, $k = 2$ allows earlier detection while relying on subsequent validation to avoid false positives.

2.1.2. Subsequent Consecutive Spike Validation

A spike event is only confirmed if the feature value exceeds θ for at least d_{min} consecutive time steps:

$$\sum_{j=0}^{d_{\text{min}}-1} \mathbb{I}[\hat{y}_{t+j} > \theta] = d_{\text{min}} \quad (3)$$

where $\mathbb{I}[\cdot]$ is the indicator function. This sustained-exceedance criterion filters out short-lived fluctuations caused by noise or transient load changes.

2.1.3. Fallback Mechanism

If the total number of validated spikes N_{spike} is below a minimum threshold n_{min} (empirically set to 5), the system returns to using the full ModernTCN prediction sequence for the estimation of RUL:

$$\text{RUL Input} = \begin{cases} \text{Features within spike window,} & N_{\text{spike}} \geq n_{\text{min}} \\ \text{Entire predicted sequence,} & N_{\text{spike}} < n_{\text{min}} \end{cases} \quad (4)$$

This ensures stable performance in cases with weak or delayed degradation signatures.

2.1.4. Advantages

The proposed adaptive thresholding with consecutive spike validation and fallback ensures robustness by reducing noise-induced false alarms, retaining only sustained degradation trends for RUL regression, or reverting to the full predicted sequence when spike evidence is insufficient.

This design improves both robustness and timeliness in detecting the onset of degradation, directly benefiting the final accuracy of the RUL regression. Consistent with the run-rules theory in Statistical Process Control (SPC) [23], we require at least $d_{\min} = 5$ consecutive spikes to validate the onset, which reduces noise-driven false alarms and preserves sensitivity to sustained degradation; otherwise, we return to full-sequence prediction.

$$\mathcal{S} = \{t \mid \hat{x}_t > \tau\}. \quad (5)$$

To be more specific, if the number of detected spikes is $|\mathcal{S}| \geq 5$, only these spike segments are retained for subsequent processing. If $|\mathcal{S}| < 5$, the algorithm comes back to using the entire predicted sequence $\{\hat{x}_t\}_{t=t_0}^{T_f}$ to ensure adequate data coverage.

This design reduces false positives from transient noise and ensures that the identified onset corresponds to a sustained degradation trend rather than a short-lived fluctuation. It also improves model robustness under cross-condition scenarios, where noise profiles can differ significantly.

2.2. Post-Onset RUL Estimation Pipeline

After detecting the onset of degradation t_s via the adaptive consecutive spike detection module, only the post-onset segment is used for RUL regression. The normalized RUL at time $t \geq t_s$ is defined as:

$$\text{RUL}_{\text{seg}}(t) = \frac{T_f - t}{T_f - t_s}, \quad (6)$$

where T_f is the failure time, ensuring $\text{RUL}_{\text{seg}}(t_s) = 1$ and $\text{RUL}_{\text{seg}}(T_f) = 0$. For each t , the feature vector \mathbf{f}_t includes the indicator predicted by ModernTCN (\hat{x}_t), the spectral slopes and peak magnitudes, the statistical derivatives (e.g., FFT_bin_2_H slope, variance, energy) and the time-domain spike metrics. These features are input to a stacking ensemble combining Random Forest (RF) and LightGBM (LGBM), with a Ridge meta-learner weighting their outputs:

$$\widehat{\text{RUL}}_{\text{seg}}(t) = \alpha \cdot \widehat{\text{RUL}}_{\text{RF}}(t) + (1 - \alpha) \cdot \widehat{\text{RUL}}_{\text{LGBM}}(t), \quad (7)$$

where α is learned from validation data. This integration takes advantage of the robustness of the RF and the efficiency of LGBM to improve the estimation of RUL.

This integration takes advantage of the robustness of RF and the efficiency of LGBM to improve RUL estimation, particularly in the post-onset prediction scenario, where precise modeling of degradation trends is critical.

2.3. Evaluation metrics

We report the mean absolute error (MAE), the root mean square error (RMSE), the coefficient of determination (R^2), and the PHM 2012 scoring function. Metrics are computed on normalized RUL series $\{y_t\}_{t=1}^m$ with predictions $\{\hat{y}_t\}_{t=1}^m$ and $\bar{y} = \frac{1}{m} \sum_{t=1}^m y_t$:

$$\text{MAE} = \frac{1}{m} \sum_{t=1}^m |y_t - \hat{y}_t|, \quad (8)$$

$$\text{RMSE} = \sqrt{\frac{1}{m} \sum_{t=1}^m (y_t - \hat{y}_t)^2}, \quad (9)$$

$$R^2 = 1 - \frac{\sum_{t=1}^m (\hat{y}_t - y_t)^2}{\sum_{t=1}^m (\bar{y} - y_t)^2}. \quad (10)$$

Following the IEEE PHM 2012 Data Challenge [24], the Score penalizes late and early predictions asymmetrically:

$$\text{Score} = \frac{1}{n-1} \sum_{t=1}^{n-1} A_t, \quad (11)$$

$$A_t = \begin{cases} \exp\left(-\ln(0.5) \frac{Er_t}{5}\right), & Er_t \leq 0, \\ \exp\left(+\ln(0.5) \frac{Er_t}{20}\right), & Er_t > 0, \end{cases} \quad (12)$$

$$Er_t = \frac{y_t - \hat{y}_t}{y_t} \times 100\%. \quad (13)$$

For completeness, a common construction of the ground-truth RUL y_t over a run of length T with first-prediction time FPT is

$$y_t = \begin{cases} T, & 0 \leq t \leq \text{FPT}, \\ T - T \frac{t - \text{FPT}}{T - \text{FPT}}, & \text{FPT} \leq t \leq T. \end{cases} \quad (14)$$

3. EXPERIMENTS

3.1. Dataset

We evaluate our framework on the XJTU-SY bearing accelerated life dataset [25], which provides run-to-failure vibration data for 15 bearings collected under three operating conditions. Each record is acquired by two orthogonal accelerometers (horizontal and vertical) at a sampling rate of 25.6 kHz, with 32 768 points per channel captured every 1 min, yielding long sequences that cover the full degradation process. For this study, we focus on the horizontal channel and use the engineered spectral indicator FFT_bin_2_H, which our Spearman analysis identified as the feature most sensitive to RUL among the available candidates.

3.2. Experimental Setup

Following the methodology described in Sec. 2, we conduct experiments on the XJTU-SY bearing dataset using a single NVIDIA GeForce RTX 3090 GPU with 24 GB memory and 18 CPU cores. The missing values in FFT_bin_2_H are removed, and the remaining useful life (RUL) is calculated as a backward count from the failure time for each bearing run.

A Modern Temporal Convolutional Network with three residual blocks ([32, 32, 16] channels) and exponentially increasing dilations (2^i) is trained in the FFT_bin_2_H feature using a sequence length $SEQ_LEN = 20$ and a prediction horizon $PRED_STEP = 5$ minutes. The model is optimized with Adam ($\eta = 10^{-3}$) and MSE loss for 10 epochs, with a batch size of 32.

4. RESULTS

4.1. Condition-Wise Evaluation with Sigma Threshold Comparison

To make a fair, like-to-like comparison with the attention-DBiLSTM (A-DBiLSTM) study by Zou et al. [9], we keep the original condition-wise train/test splits on XJTU-SY and evaluate post-onset segmentation and full-length modes (Table 2). Think of the protocol as a controlled trial: we ask both methods to run the same course, then watch what happens when faults begin. Across the three operating conditions, SARNet enters the post-onset window earlier and steadily, turning energy spikes into actionable triggers

Table 2: Performance under segmentation and full-length evaluation for all test bearings.

Test Bearing	k_σ	Segmentation Mode				Full-length Mode			
		RMSE	MAE	R^2	MAPE	RMSE	MAE	R^2	MAPE
bearing1_3	2	0.0308	0.0196	0.9888	661.30	0.0486	0.0291	0.9720	480.03
bearing1_3	3	0.0400	0.0232	0.9811	405.65	0.0587	0.0349	0.9591	296.95
bearing2_5	2	0.0337	0.0190	0.9865	1377.31	0.0692	0.0329	0.9429	1192.20
bearing2_5	3	0.0367	0.0207	0.9839	1121.56	0.0687	0.0339	0.9438	971.15
bearing3_5	2	0.0754	0.0564	0.9332	8236.07	0.1049	0.0747	0.8702	5129.44
bearing3_5	3	0.0678	0.0513	0.9461	6615.39	0.0972	0.0686	0.8886	4120.97

Table 3: Ablation of the proposed SAR (Spike-Aware) framework. Spike-aware variants (top) consistently improve R^2 / RMSE despite lower coverage (fewer, high-signal windows). Best model in bold.

Method	RMSE	MAE	R^2	Coverage	Learner	# of Feature
<i>SAR Framework (Spike-Aware Detection + MTCN backbone)</i>						
SARNet	0.036187	0.020585	0.989434	118	ENS	9
SAR + RF	0.037329	0.014730	0.988756	118	RF	9
SAR + LGBM	0.044625	0.029210	0.983931	118	LGBM	9
SAR (linear head)	0.312706	0.263490	0.210959	118	Linear	1
<i>Ablations without Spike-Aware Detection (MTCN backbone only)</i>						
MTCN + LGBM	0.067023	0.043393	0.946094	1833	LGBM	9
MTCN + RF-LGBM	0.075449	0.046989	0.931689	1833	ENS	9
MTCN + RF	0.088960	0.054662	0.905033	1833	RF	9
MTCN (linear head)	0.288225	0.251415	0.003116	1833	Linear	1

rather than noise; the result is a materially lower error and higher R^2 than A-DBiLSTM without sacrificing whole-sequence reporting. Concretely, under the same splits, SARNet’s *segmentation* mode cuts error markedly relative to A-DBiLSTM: RMSE drops by about 55% in Condition 1, 58% in Condition 2, and 22% in Condition 3. Averaged across the three conditions, this is a 45% reduction in RMSE; MAE follows the same pattern with reductions of roughly 74%, 68%, and a modest 4% in the hardest setting. The full-length mode remains favorable in two conditions and within range in the third, but the gain primarily comes from spike-aware segmentation. The takeaway is straightforward: Once the onset is validated, spike-aware selection reduces variance, dampens false alarms, and stabilizes predictions, giving practitioners a clearer picture of remaining life while preserving traceability to the raw signal. And avoids overfitting to condition shifts seen in practice.

The other takeaway is also intuitive. Using $\sigma = 2$ with SAR framework produces markedly lower errors than $\sigma = 3$, substantially improving the predictive capacity of the model. This confirms that our refinement of the 3σ rule is reasonable and effective. In practice, the tighter threshold captures incipient spikes earlier and reduces variance in the post onset window. It also reduces false alarms while keeping the predictions traceable to the original signal.

4.2. Ablation Study

Table 3 presents the ablation study. The spike aware selection combined with the ModernTCN backbone produces consistent gains regardless of the regression head. The best variant, **SARNet**, which averages the predictions of Random Forest and LightGBM, achieves a 0.036 RMSE, 0.021 MAE, and approximately 99 percent R^2 . Using a single head remains competitive, but is weaker: SAR with Random Forest achieves RMSE 0.037329 and R^2 0.988756, and SAR with LightGBM reaches RMSE 0.044625 and R^2 0.983931. A linear head under the same backbone performs poorly, which underlines the need for a nonlinear regressor in the post onset regime.

When spike aware detection is removed, the accuracy drops markedly even though many more windows are used. The strongest non-spoke baseline (MTCN with LightGBM) yields RMSE 0.067 and R^2 0.946. Compared to this baseline, SARNet reduces RMSE by approximately **46%** and increases R^2 by approximately **0.043**. Notably, SAR variants operate on 118 post-onset windows on average, whereas the full length mode uses 1833 windows. This corresponds to about fifteen times fewer inputs while delivering

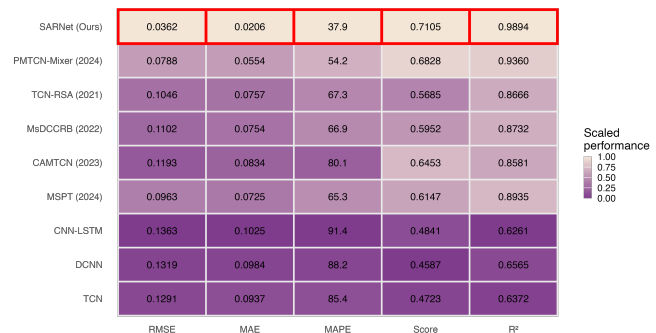


Fig. 2: Comparison with representative baselines (baselines numbers from [8]); our results follow the same protocol.

better accuracy, which is attractive for real time use.

4.3. Comparison with Previous Researches

Figure 2 compares the SARNet with representative predictors of RUL bearings from recent years. Under the same experimental protocol and evaluation metrics (RMSE, MAE, MAPE, and R^2), our approach remains lightweight while achieving better performance, with consistently higher R^2 and lower RMSE, MAE, and MAPE than competing methods.

In general, three conclusions emerge.

- The **Post onset evaluation is preferable**, as the concentration of the assessment on post onset segments consistently outperforms the full sequence scoring across bearings and metrics.
- **Spike-Aware detection is the main driver**, which yields substantial gains even before the downstream regressor is chosen.
- The **RF-LGBM Ensemble is the most reliable combination** within the SAR family, combining Random Forest and LightGBM produces the most stable and accurate post-onset RUL estimates, while preserving interpretability and ease of deployment.

5. CONCLUSION

SARNet demonstrates reliable remaining useful life prediction across the XJTU-SYbearings with consistent gains in accuracy and stability. The framework couples a ModernTCN forecaster with an adaptive consecutive spike validator, which suppresses noise while preserving abrupt degradation cues that are often diluted by end to end sequence models. Because the validator adapts to each run and condition, the method remains effective without requiring matched data across operating regimes and is therefore well suited to resource constrained deployments.

The proposed model outperforms recent convolutional and recurrent baselines. In segmentation mode, it yields roughly a one half reduction in RMSE and a sixty percent reduction in MAE relative to a strong ModernTCN Mixer baseline, while achieving an R^2 close to 0.99. These improvements arrive with clear feature attributions from the RF and LightGBM head and a small computational footprint that runs comfortably on a CPU. This progress not only lowers the deployment cost for enterprises, it also makes the model’s predictive mechanism easier to understand.

Overall, SARNet offers a practical, lightweight, and transparent alternative to black box deep networks for industrial prognostics, maintaining the degradation characteristics needed for precise post onset RUL estimation while remaining easy to interpret and deploy.

6. REFERENCES

- [1] Carlos Ferreira and Gil Gonçalves, “Remaining useful life prediction and challenges: A literature review on the use of machine learning methods,” *Journal of Manufacturing Systems*, vol. 63, pp. 550–562, Apr. 2022.
- [2] Yaguo Lei, Tianyu Han, Biao Wang, Naipeng Li, Tao Yan, and Jun Yang, “XJTU-SY rolling element bearing accelerated life test datasets: A tutorial,” *Journal of Mechanical Engineering*, vol. 55, pp. 1, 08 2019.
- [3] L. Magadán, J. C. Granda, and F. J. Suárez, “Robust prediction of remaining useful lifetime of bearings using deep learning,” *Engineering Applications of Artificial Intelligence*, vol. 130, pp. 107690, Apr. 2024.
- [4] Yifei Ding, Minping Jia, and Yudong Cao, “Remaining useful life estimation under multiple operating conditions via deep subdomain adaptation,” *IEEE Transactions on Instrumentation and Measurement*, vol. 70, pp. 1–11, 2021.
- [5] Yifei Ding, Peng Ding, Xiaoli Zhao, Yudong Cao, and Minping Jia, “Transfer learning for remaining useful life prediction across operating conditions based on multisource domain adaptation,” *IEEE/ASME Transactions on Mechatronics*, vol. 27, no. 5, pp. 4143–4152, 2022.
- [6] Cheng-Geng Huang, Hong-Zhong Huang, and Yan-Feng Li, “A bidirectional LSTM prognostics method under multiple operational conditions,” *IEEE Transactions on Industrial Electronics*, vol. 66, no. 11, pp. 8792–8802, 2019.
- [7] Xianhua Chen and Zhigang Tian, “A novel method for identifying sudden degradation changes in remaining useful life prediction for bearing,” *Expert Systems with Applications*, vol. 278, pp. 127315, June 2025.
- [8] Dechen Yao, Bo Tang, Jianwei Yang, Wenbo Yue, Qiang Li, and Shudong Guo, “Patch ModernTCN-Mixer: a dual-task temporal convolutional network framework for hybrid implementation of first prediction time detection and remaining useful life prognosis,” *Measurement Science and Technology*, vol. 35, no. 11, pp. 116011, Nov. 2024.
- [9] Yi Zou, Wenlei Sun, Hongwei Wang, Tiantian Xu, and Bingkai Wang, “Research on bearing remaining useful life prediction method based on double bidirectional long short-term memory,” *Applied Sciences*, vol. 15, no. 8, pp. 4441, Apr. 2025.
- [10] Shaojie Bai, J. Zico Kolter, and Vladlen Koltun, “An empirical evaluation of generic convolutional and recurrent networks for sequence modeling,” *arXiv preprint arXiv:1803.01271*, Apr. 2018.
- [11] Lei Yang, Yibo Jiang, Kang Zeng, and Tao Peng, “Rolling bearing remaining useful life prediction based on CNN-VAE-MBiLSTM,” *Sensors*, vol. 24, no. 10, pp. 2992, 2024.
- [12] Haobo Qiu, Yingchun Niu, Jie Shang, Liang Gao, and Danyang Xu, “A piecewise method for bearing remaining useful life estimation using temporal convolutional networks,” *Journal of Manufacturing Systems*, vol. 68, pp. 227–241, June 2023.
- [13] Guangjun Jiang, Zhengwei Duan, Qi Zhao, Dezh Li, and Yu Luan, “Remaining useful life prediction of rolling bearings based on TCN-MSA,” *Measurement Science and Technology*, vol. 35, no. 2, pp. 025125, Feb. 2024.
- [14] C. Zhang, M. Zeng, J. Fan, and X. Li, “Application of residual structure time convolutional network based on attention mechanism in remaining useful life interval prediction of bearings,” *Sensors*, vol. 24, no. 13, pp. 4132, June 2024.
- [15] Jehn-Ruey Jiang, Juei-En Lee, and Yi-Ming Zeng, “Time series multiple channel convolutional neural network with attention-based long short-term memory for predicting bearing remaining useful life,” *Sensors*, vol. 20, no. 1, pp. 166, 2020.
- [16] Sheng Zhang and Zhang Wu, “Designs of control charts with supplementary runs rules,” *Computers & Industrial Engineering*, vol. 49, no. 1, pp. 76–97, Aug. 2005.
- [17] Luca Biggio, Alexander Wieland, Manuel Arias Chao, Iason Kastanis, and Olga Fink, “Uncertainty-aware remaining useful life predictor,” *arXiv*, 2021.
- [18] Ripan Kumar Kundu and Khaza Anuarul Hoque, “Explainable predictive maintenance is not enough: Quantifying trust in remaining useful life estimation,” in *Proceedings of the Annual Conference of the PHM Society*, Oct. 2023, vol. 15.
- [19] Oscar Serradilla, Ekhi Zugasti, and Urko Zurutuza, “Deep learning models for predictive maintenance: a survey, comparison, challenges and prospect,” *arXiv preprint arXiv:2010.03207*, Oct. 2020.
- [20] Olga Fink, Qin Wang, Markus Svensén, Pierre Dersin, Wan-Jui Lee, and Melanie Ducoffe, “Potential, challenges and future directions for deep learning in prognostics and health management applications,” *arXiv preprint arXiv:2005.02144*, May 2020.
- [21] Donghao Luo and Xue Wang, “ModernTCN: A modern pure convolution structure for general time series analysis,” in *The Twelfth International Conference on Learning Representations*, 2024.
- [22] Rüdiger Lehmann, “ 3σ -rule for outlier detection from the viewpoint of geodetic adjustment,” *Journal of Surveying Engineering*, vol. 139, no. 4, pp. 157–165, Nov. 2013.
- [23] Jungtaek Oh and Christian H. Weiß, “On the individuals chart with supplementary runs rules under serial dependence,” *Methodology and Computing in Applied Probability*, vol. 22, no. 3, pp. 1257–1273, Sept. 2020.
- [24] Patrick Nectoux, Rafael Gouriveau, Kamal Medjaher, Emmanuel Ramasso, Brigitte Morello, Nourredine Zerhouni, and Christophe Varnier, “Pronostia: An experimental platform for bearings accelerated life test,” in *Proceedings of the IEEE International Conference on Prognostics and Health Management (PHM)*, Denver, CO, USA, 2012.
- [25] Biao Wang, Yaguo Lei, Naipeng Li, and Ningbo Li, “A hybrid prognostics approach for estimating remaining useful life of rolling element bearings,” *IEEE Transactions on Reliability*, vol. 69, no. 1, pp. 401–412, 2020.